The current issue and full text archive of this journal is available at
www.emeraldinsight.com/0961-5539.htm

On steady MHD flow and heat transfer past a rotating disk in a porous medium with ohmic heating and viscous dissipation

P. Sibanda
School of Mathematical Sciences, University of KwaZulu-Natal, Pietermaritzburg, South Africa, and
O.D. Makinde
Faculty of Engineering, Cape Peninsula University of Technology, Bellville, South Africa

Received 16 April 2009
Accepted 12 June 2009

Abstract

Purpose – The purpose of this paper is to investigate the hydromagnetic steady flow and heat transfer characteristics of an incompressible viscous electrically conducting fluid past a rotating disk in a porous medium with ohmic heating, Hall current and viscous dissipation are also investigated.
Design/methodology/approach – Using appropriate similarity variables and boundary-layer approximations, the fluid equations for continuity, momentum and energy balance governing the problem are formulated. These equations are solved numerically by using the most effective Newton-Raphson shooting method along with fourth-order Runge-Kutta integration algorithm.
Findings – It was found that magnetic field retards the fluid motion due to the opposing Lorentz force generated by the magnetic field. Both the magnetic field and the Eckert number tend to enhance the heat transfer efficiency. The Hall parameter however reduces the heat transfer rate. In terms of the friction coefficient, the magnetic interaction parameter, the Hall parameter and the Eckert number all combine to increase the skin friction, while increasing the Darcy number (increasing permeability) reduces the skin friction so increasing the fluid velocity.
Practical implications – This paper provides a very useful source of information for researchers on the subject of hydromagnetic flow in porous media.
Originality/value – This type of problem has potential to serve as a prototype for practical swirl problems, for example, axisymmetric flow in combustors.

Keywords Electric current, Magnetic fields, Porous materials, Flow, Heat transfer, Viscosity
Paper type Research paper

Nomenclature

B_0	magnetic flux density
C_p	specific heat at constant pressure
Da	local Darcy number, $K\Omega/\upsilon$
Ec	Eckert number, $r^2\Omega^2/\rho\Delta T$
F	non-dimensional radial velocity
G	non-dimensional tangential velocity
g	acceleration due to gravity
G_r	Modified Grashof number, $g\beta(T_w - T_\infty)/\sqrt{\upsilon\Omega^3}$
H	non-dimensional axial velocity
H_w	non-dimensional injection/suction velocity, $W/\sqrt{\upsilon\Omega}$
K	Darcy permeability parameter

The authors thank the National Research Foundation and the NRF Thuthuka program for financial support.

0961-5539
DOI 10.1108/09615531011024039

M magnetic interaction parameter, $\sigma B_0^2/\rho\Omega$
p fluid pressure
Pr Prandtl number, $\mu C_p/\kappa$
Re rotational Reynolds number, $r^2\Omega/\upsilon$
s Hall parameter
T fluid temperature
T_w disk temperature
T_∞ ambient fluid temperature
u radial velocity
v tangential velocity
W uniform suction/injection velocity
w axial velocity
r radial axis
z vertical axis

Greek symbols
β coefficient of thermal expansion
ξ normal distance from the disk
θ non-dimensional temperature
κ thermal conductivity coefficient
μ dynamic viscosity
υ kinematic viscosity
φ tangential axis
ρ fluid density
σ electrical conductivity
Ω angular velocity

1. Introduction

The problem of hydrodynamic stability of flow due to a rotating disk is of great interest in many engineering fields, particularly in the care and maintenance of turbine engines and other rotary type machine systems, Arikoglu and Ozkol (2006). Typically, such flows may be subjected to high operating temperatures and keeping an accurate map of the velocity and temperature fields is necessary to ensure optimal operation of the machinery. Finding the solutions of the highly non-linear and coupled governing however remained an intractable problem until the pioneering work of von Karman (1921) in which he introduced self-similar transformations that reduced the governing partial differential equations to be reduced to ordinary differential equations that could be solved using an approximate integral method.

The early study by von Karman has since been considerably improved and extended, starting with the work of Cochran (1934) who improved von Karman's results by using a Taylor series expansion near the disk and a series solution involving exponentially decaying functions far from the disk. Extensions to the earlier work have included, *inter alia*, finding the effects of:

- impulsively starting the flow from rest (Benton, 1966; Rogers and Lance, 1960);
- an axial magnetic field applied to the fluid with or without Hall effects (El-Mistikawy *et al.*, 1990; Attia and Aboul-Hassan, 2004); and
- variable fluid properties (Herwig, 1985; Herwig and Klemp, 1988; Maleque and Sattar, 2005).

Other recent studies on various aspects of the rotating disk flow problem include the works of Takha *et al.* (2002) who considered electrically conducting fluids in magnetohydrodynamics (MHD) flow and Arikoglu and Ozkol (2006) who considered heat transfer characteristics on MHD flow.

The series of studies by Attia (2004, 2006, 2007) considered the effects of:

- ion slip;

- temperature-dependent viscosity; and
- ohmic heating on rotating disk flow.

The present study incorporates the effects of ohmic and viscous heat dissipation, Hall currents, porosity and an applied magnetic field on rotating disk flow with constant properties. Recent studies on rotating disk flow that provide the basis for this work include those of Osalusi and Sibanda (2006) who considered variable property laminar convective flow due to a porous disk, Frusteri and Osalusi (2007) who considered ion-slip effects in rotating disk with variable properties and Osalusi *et al.* (2007) who considered ohmic heating, viscous dissipation, Hall and ion-slip currents in MHD flow over a porous rotating disk with variable. There is an extensive literature on the general problem of flow subject to an applied electromagnetic field, see for example, Makinde (2005) and Makinde and Sibanda (2008).

2. Mathematical formulation

Consider non-rotating cylindrical polar coordinates (r, φ, z) where z is the vertical axis with r and φ as the radial and tangential axes, respectively. The disk rotates with constant angular velocity Ω about the z-axis in a viscous incompressible electrically conducting Newtonian fluid in a porous medium. The components of the flow velocity are u, v and w in the directions of increasing r, φ and z, respectively. The fluid pressure is p, the density of the fluid is ρ and T is the fluid temperature. The surface of the rotating disk is maintained at a uniform temperature T_w while the temperature of the ambient fluid is T_∞.

An external uniform magnetic field is applied perpendicular to the surface of the disk and has a constant magnetic flux density B_0 with a small magnetic Reynolds number so that the induced magnetic field is small in comparison with the applied magnetic field. Under the Boussinesq approximation, the basic equations governing the flow of the fluid in the presence of the porous medium are:

$$\frac{\partial u}{\partial r} + \frac{u}{r} + \frac{\partial w}{\partial z} = 0, \tag{1}$$

$$\begin{aligned} u\frac{\partial u}{\partial r} + w\frac{\partial u}{\partial z} - \frac{v^2}{r} + \frac{\upsilon}{K}u = -\frac{1}{\rho}\frac{\partial p}{\partial r} + \upsilon\left(\frac{\partial^2 u}{\partial r^2} + \frac{1}{r}\frac{\partial u}{\partial r} - \frac{u}{r^2} + \frac{\partial^2 u}{\partial z^2}\right) \\ - \frac{\sigma B_0^2}{\rho(1+s^2)}(u - sv), \end{aligned} \tag{2}$$

$$u\frac{\partial v}{\partial r} + \frac{uv}{r} + w\frac{\partial v}{\partial z} + \frac{\upsilon}{K}v = \upsilon\left(\frac{\partial^2 v}{\partial r^2} + \frac{1}{r}\frac{\partial v}{\partial r} - \frac{v}{r^2} + \frac{\partial^2 v}{\partial z^2}\right) - \frac{\sigma B_0^2}{\rho(1+s^2)}(v + su), \tag{3}$$

$$u\frac{\partial w}{\partial r} + w\frac{\partial w}{\partial z} + \frac{\upsilon}{K}w = -\frac{1}{\rho}\frac{\partial p}{\partial z} + \upsilon\left(\frac{\partial^2 w}{\partial r^2} + \frac{1}{r}\frac{\partial w}{\partial r} + \frac{\partial^2 w}{\partial z^2}\right) + g\beta(T - T_\infty), \tag{4}$$

where σ is the electrical conductivity, g is acceleration due to gravity, β is the coefficient of thermal expansion, K is the Darcy permeability parameter and s is the Hall parameter which may be positive or negative depending on the orientation of the magnetic field.

The energy equation describing the temperature distribution in the fluid that incorporates ohmic and viscous dissipation is:

$$u\frac{\partial T}{\partial r}+w\frac{\partial T}{\partial z}=\frac{\kappa}{\rho C_p}\left(\frac{\partial^2 T}{\partial r^2}+\frac{1}{r}\frac{\partial T}{\partial r}+\frac{\partial^2 T}{\partial z^2}\right)+\frac{2\upsilon}{C_p}\left\{\left(\frac{\partial u}{\partial r}\right)^2+\frac{u^2}{r^2}+\left(\frac{\partial w}{\partial z}\right)^2\right\}$$
$$+\frac{\upsilon}{C_p}\left\{\left(\frac{\partial v}{\partial z}\right)^2+\left(\frac{\partial w}{\partial r}+\frac{\partial u}{\partial z}\right)^2+\left[r\frac{\partial}{\partial r}\left(\frac{v}{r}\right)\right]^2\right\}+\frac{\sigma B_0^2}{\rho C_p}(u^2+v^2), \tag{5}$$

where T is the temperature of the fluid, C_p is the specific heat at constant pressure and k is the thermal conductivity of the fluid. The last three terms in Equation (5) represent viscous and ohmic dissipation, respectively. A major difference between this work and the earlier studies by Attia (2004), Attia and Aboul-Hassan (2004) and Attia (2007) is the inclusion of both ohmic and viscous dissipation in the current study. Joule and viscous dissipation effects are included in Attia (2005), which, however is a separate study on Couette rather than rotating disk flow.

The boundary conditions for the flow are:

$$\begin{aligned} &z=0:\ u, \quad w=W, \quad v=r\Omega, \quad T=T_\infty, \\ &z\to\infty:\ u, \quad v\to 0, \quad T\to T_\infty, \quad p\to p_\infty, \end{aligned} \tag{6}$$

where the subscript "∞" denotes ambient conditions. The following von Karman similarity transformations (see Attia, 2007) are now introduced:

$$\begin{aligned} &F=\frac{u}{r\Omega}, \quad G=\frac{v}{r\Omega}, \quad H=\frac{w}{\sqrt{\upsilon\Omega}}, \\ &\theta=\frac{T-T_\infty}{\Delta T}, \quad \xi=z\sqrt{\Omega/\upsilon}, \quad P=\frac{p-p_\infty}{\rho\upsilon\Omega}, \end{aligned} \tag{7}$$

where $\Delta T = T_w - T_\infty$, ξ is a non-dimensional distance along the axis of rotation, υ is the kinematic viscosity of the fluid, F, G and H are the non-dimensional radial, tangential and axial velocity components.

Using the above transformations, Equations (1)-(5) reduce to:

$$H'+2F=0, \tag{8}$$

$$F''-HF'-F^2+G^2-Da^{-1}F-\frac{M}{1+s^2}(F-sG)=0, \tag{9}$$

$$G''-HG'-2FG-Da^{-1}G-\frac{M}{1+s^2}(G+sF)=0, \tag{10}$$

$$H''-HH'+P'-Da^{-1}H+G_r\theta=0, \tag{11}$$

$$\frac{1}{Pr}\theta''-H\theta'+\frac{2Ec}{Re}[(H')^2+2F^2]+Ec[(G')^2+(F')^2]+MEc(F^2+G^2)=0. \tag{12}$$

The physical parameters appearing in Equations (8)-(12) are defined as follows:

$$Da = \frac{K\Omega}{\upsilon}, \quad M = \frac{\sigma B_0^2}{\rho\Omega}, \quad G_r = \frac{g\beta(T_w - T_\infty)}{\sqrt{\upsilon\Omega^3}}, \quad Ec = \frac{r^2\Omega^2}{C_p\Delta T}, \quad Re = \frac{r^2\Omega}{\upsilon}, \quad (13)$$

where Da is the local Darcy number, Ec is the Eckert number that characterizes dissipation, G_r is a modified Grashof number, M is the magnetic interaction parameter, Re is the local rotational Reynolds number and $Pr = \mu C_p/\kappa$ is the Prandtl number. The appropriate boundary conditions are:

$$F(0) = 0, \quad H(0) = H_w, \quad G(0) = \theta(0) = 1 \quad \text{at}\ \xi = 0, \quad (14)$$

$$F(\xi) = H(\xi) = G(\xi) = \theta(\xi) = 0 \quad \text{as}\ \xi \to \infty, \quad (15)$$

where $H_w = W/\sqrt{\upsilon\Omega}$ is the suction ($H_w < 0$) or injection ($H_w > 0$) velocity at the disk surface.

3. Computational method

The numerical technique chosen for the solution of the coupled ordinary differential Equations (8)-(12) is the standard Newton–Raphson shooting method along with a fourth-order Runge–Kutta integration algorithm. Equations (8)-(12) are transformed into a system of first-order differential equations as follows. Let $F = x_1$, $F' = x_2$, $H = x_3$, $H' = x_4$, $G = x_5$, $G' = x_6$, $\theta = x_7$, $\theta' = x_8$ where the prime represent derivatives with respect to ξ. Then:

$$\begin{aligned}
x_1' &= x_2, \\
x_2' &= x_2x_3 + x_1^2 - x_5^2 + Da^{-1}x_1 + \frac{M(x_1 - sx_5)}{(1+s^2)}, \\
x_3' &= x_4, \\
x_4' &= x_3x_4 + Da^{-1}x_3 - G_r x_7, \\
x_5' &= x_6, \\
x_6' &= x_3x_6 + 2x_1x_5 + Da^{-1}x_5 + \frac{M(x_5 + sx_1)}{(1+s^2)}, \\
x_7' &= x_8, \\
x_8' &= Prx_3x_8 - \frac{2PrEc}{Re}(x_4^2 + 2x_1^2) - PrEc[(x_6^2 + x_2^2) + M(x_1^2 + x_5^2)],
\end{aligned} \quad (16)$$

subject to the following initial conditions,

$$\begin{aligned}
&x_1(0) = 0, \quad x_2(0) = s_1, \quad x_3(0) = s_5, \quad x_4(0) = s_2, \\
&x_5(0) = 1, \quad x_6(0) = s_3, \quad x_7(0) = 1, \quad x_8(0) = s_4.
\end{aligned} \quad (17)$$

The unspecified initial conditions s_1, s_2, s_3 and s_4 are guessed systematically and Equations (16) are then integrated numerically as initial valued problems to a given terminal point. The procedure was repeated until the results we obtained up to the desired degree of accuracy, namely 10^{-7}. The value of ξ_∞ was found for each iteration loop by the assignment statement $\xi_\infty = \xi_\infty + \Delta\xi$. The maximum value of ξ_∞ to each group of parameters M, Pr, G_r, Da, s, Re and Ec was determined when the values of unknown boundary conditions at $\xi = 0$ did not change in successive loops with error more than 10^{-7}.

4. Results and discussion

The numerical calculations for the local skin friction and the heat transfer rates are presented in Table I. Figures 1-19 present the variation of the non-dimensional velocity and temperature profiles with different parameter values. Numerical computations were carried out for a fixed Prandtl number, $Pr = 0.71$, that corresponds to air.

The boundary conditions (15) imply that all the velocity components and the fluid temperature vanish at sufficiently large distances from the disk surface. These conditions differ from those used in Frusteri and Osalusi (2007) and Osalusi *et al.* (2007) where the axial velocity approaches a numerically determined asymptotic limit. In addition, in the two aforementioned studies, analysis of the results is limited to the suction case ($H_w < 0$). In this study we consider the case of small uniform injection ($0 < H_w < 1$) and moderate rotational Reynolds numbers.

Table I shows the effect of parameter variation on the skin friction and the rate of heat transfer at the disk surface. The radial skin friction and the heat transfer rate increases with increasing values of M. This is however contrary to the findings in Osalusi *et al.* (2007) where they considered the case of variable fluid properties in the presence of Hall, ion-slip currents and suction, and showed that both the radial skin friction and the rate of heat transfer decreases with increases in M. This discrepancy can be explained by the findings in Frusteri and Osalusi (2007) that increasing the ion-slip factor (absent in our study) significantly reduces both the skin friction coefficients and the heat transfer rate. Similarly, their results show that the skin friction reduces with increasing Eckert numbers while our finding is that for moderate injection, the skin friction in the radial and axial directions increases with Eckert numbers.

Furthermore, the skin friction coefficients and the heat transfer rate increase with the Hall parameter s (which is in line with the findings in Osalusi *et al.*, 2007), as well as increases in G_r and Da.

The rate of heat transfer increases with increasing Hartmann numbers M, Eckert number Ec, the modified Grashof number G_r and the Darcy number Da.

M	s	G_r	Da	Ec	$F'(0)$	$H'(0)$	$G'(0)$	$-\theta'(0)$
0.1	1.0	0.10	10	0.1	0.558516194	0.1959449684	−0.59295067	0.0761095069
1.0	1.0	0.10	10	0.1	0.612960069	0.1927945625	−0.90418024	0.0763706781
1.5	1.0	0.10	10	0.1	0.647846880	0.1922430699	−1.04563889	0.0808289319
1.0	1.5	0.10	10	0.1	0.646563289	0.1941631669	−0.82319066	0.0817923379
1.0	2.0	0.10	10	0.1	0.653489782	0.1951805572	−0.76583218	0.0849265047
1.0	1.0	0.12	10	0.1	0.615252072	0.2272746291	−0.89929007	0.0788654279
1.0	1.0	0.14	10	0.1	0.617338940	0.2600121207	−0.89469781	0.0811045462
1.0	1.0	0.10	2	0.1	0.523289180	0.0621147521	−1.07163943	0.0367705162
1.0	1.0	0.10	1	0.1	0.449339574	−0.0024958467	−1.25697567	0.2420446356
1.0	1.0	0.10	10	1.0	0.618437179	0.25792450699	−0.89366671	0.8302957456
1.0	1.0	0.10	10	1.5	0.621496486	0.29613119641	−0.88752709	1.3071470936
1.0	1.0	0.10	10	2.0	0.624608190	0.33658925148	−0.88105099	1.8407554671

Table I.
Skin friction values of $F'(0)$, $H'(0)$, $G'(0)$ and heat transfer rates $\theta'(0)$ for $H_w = 0.1$, $Re = 1$, $Pr = 0.71$

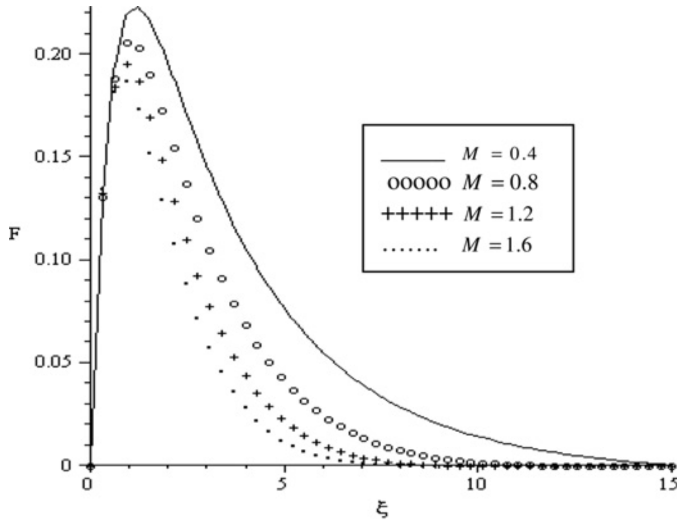

Notes: $Ec = 0.1$, $G_r = 0.1$, $Re = 1$, s = 1, $H_w = 0.1$ and $Da = 10$

Figure 1.
The effect of increasing the magnetic interaction parameter on the radial velocity

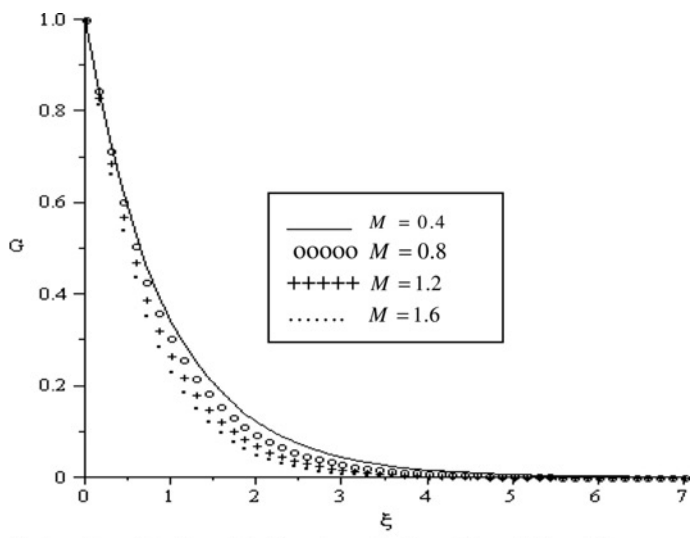

Notes: $Ec = 0.1$, $G_r = 0.1$, $Re = 1$, s = 1, $H_w = 0.1$ and $Da = 10$

Figure 2.
Effect of varying the magnetic interaction parameter on the steady tangential velocity

4.1 Effect of the magnetic interaction

Figures 1 and 2 show the effect of increasing the magnetic interaction parameter M on the steady-state radial and tangential velocity components respectively when the other governing flow parameters are held constant. The numerical simulations show that, even in the presence of (moderate) injection, the magnetic field suppresses the fluid velocity. In order to satisfy the continuity equation, the axial velocity component is also be suppressed. The decrease in the velocity is accompanied by an increase in the

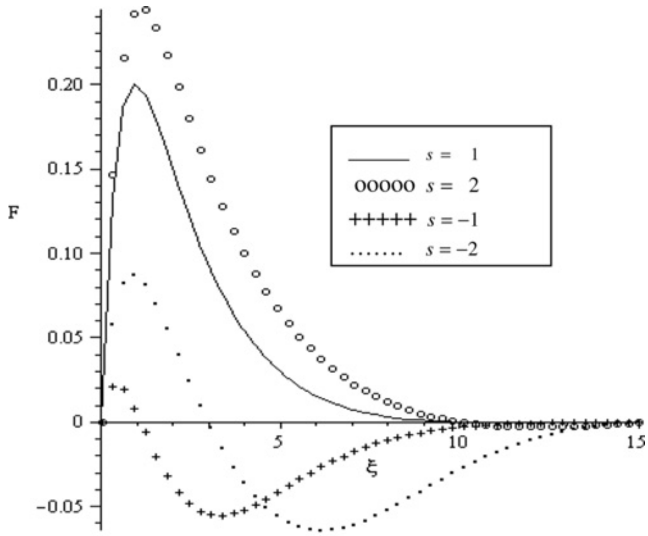

Notes: $Ec = 0.1$, $G_r = 0.1$, $Re = 1$, $M = 1$, $H_w = 0.1$ and $Da = 10$

Figure 3.
The effect of varying the Hall current s on the radial velocity

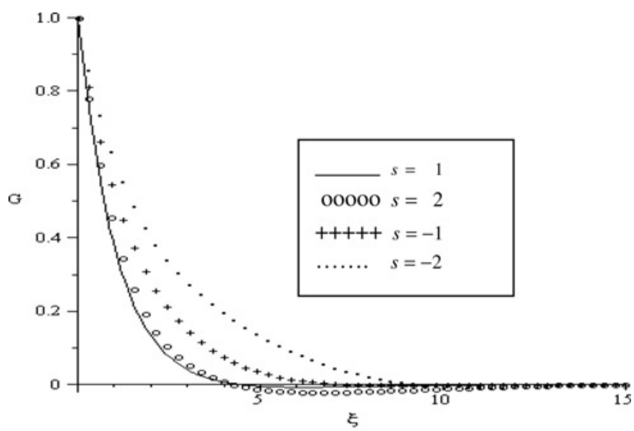

Notes: $Ec = 0.1$, $G_r = 0.1$, $Re = 1$, $M = 1$, $H_w = 0.1$ and $Da = 10$

Figure 4.
The effect of varying the Hall current s on the steady tangential velocity

temperature and the warming up of the fluid as it passes over the disk, Osalusi *et al.* (2007).

The decrease in the radial velocity seen in Figure 1 is also in line with the increase in the skin friction coefficient observed in Table I. The boundary layer thickness decreases as the magnetic field effect increases.

4.2 Effect of the Hall current

Figures 3-5 present the effects of increasing the Hall parameter s on the velocity profiles when the magnetic interaction parameter $M = 1$ is held constant. The effect of s is intricately linked to M since $M = 0$ implies the absence of the Hall effects. For large

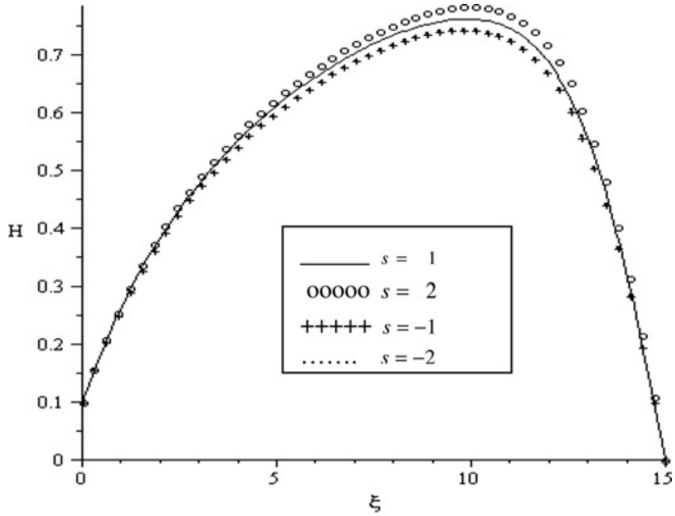

Notes: $Ec = 0.1$, $G_r = 0.1$, $Re = 1$, $M = 1$, $H_w = 0.1$ and $Da = 10$

Figure 5.
The effect of varying the Hall current s on the axial velocity

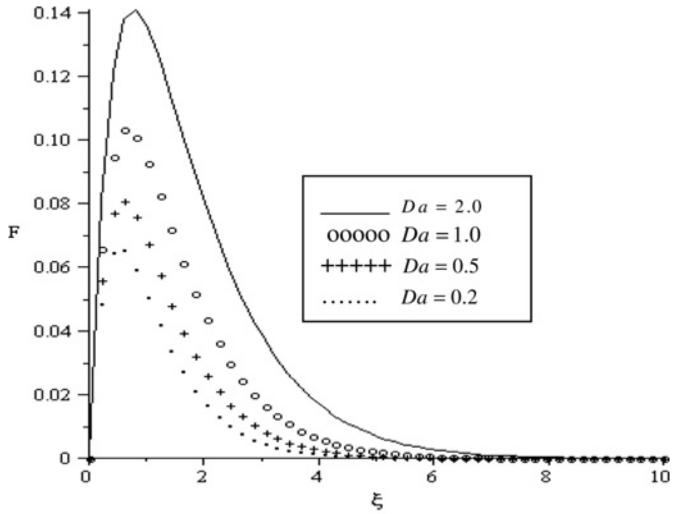

Notes: $Ec = 0.1$, $G_r = 0.1$, $Re = 1$, $M = 1$, $H_w = 0.1$ and $s = 1$

Figure 6.
Radial velocity component for different Darcy number

values of M and $s \approx O(1)$ (such that $M >> 1 + s^2$), the magnetic interaction parameter has a much greater impact on the flow characteristics than the Hall parameter. However, as in Attia and Aboul-Hassan (2004), for some non-zero values of the Hall parameter, the velocity difference $F - sG$ may well be negative. In such a case, the magnetic field would be propelling rather than retarding the flow. Figure 3 shows that flow reversal (also seen in Attia and Aboul-Hassan, 2004) is possible for negative values of s. For large negative s the minimum velocity appears further and further from the disk surface. In Figure 4, negative values of s actually enhance the tangential velocity by reducing the effective magnetic damping (Attia, 2004).

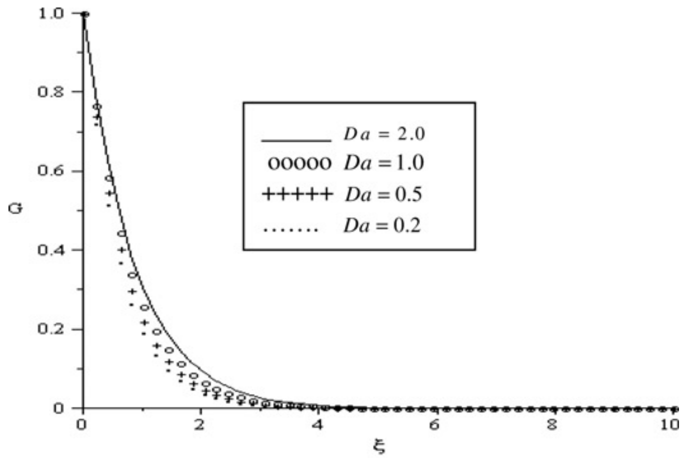

Notes: $Ec = 0.1$, $G_r = 0.1$, $Re = 1$, $M = 1$, $H_w = 0.1$ and $s = 1$

Figure 7.
Change in the tangential velocity for different Darcy numbers

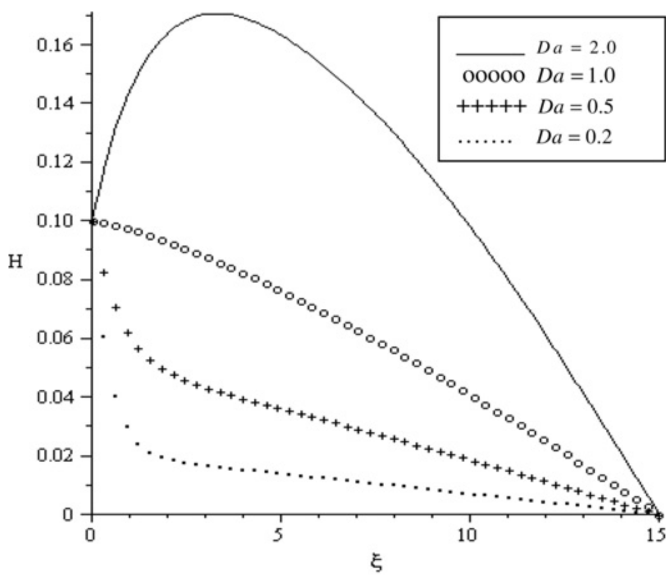

Notes: $Ec = 0.1$, $G_r = 0.1$, $Re = 1$, $M = 1$, $H_w = 0.1$ and $s = 1$

Figure 8.
Change in the axial velocity for different Darcy numbers

Back flow occurs for large positive Hall parameter values caused by the strong magnetic deceleration of the fluid in Equation (10).

In Figure 5, the effect of reducing s is to produce only a marginal reduction in the maximum value of the axial velocity component. Overall, the effect of an increase in the Hall parameter is to increase the fluid velocity while conversely reducing the temperature. This result is again consistent with the earlier results (for example, Osalusi *et al.*, 2007), and shows that moderate injection or suction does not significantly change the characteristics of rotating disk flow.

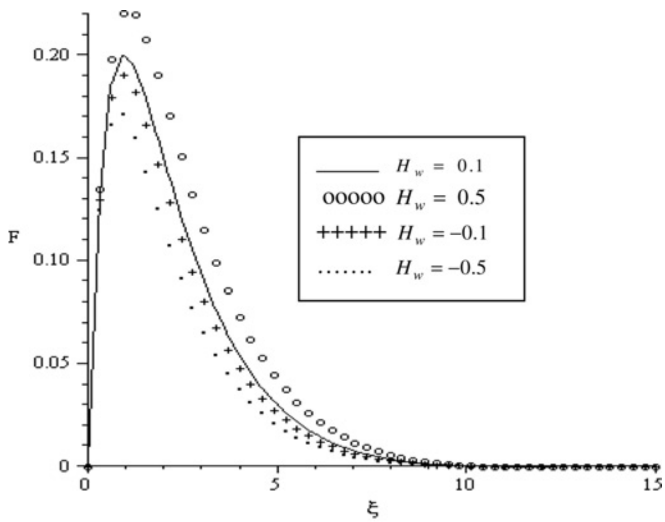

Notes: $Ec = 0.1$, $G_r = 0.1$, $Re = 1$, $M = 1$, $Da = 10$ and $s = 1$

Figure 9. Effect of varying H_w on radial velocity component

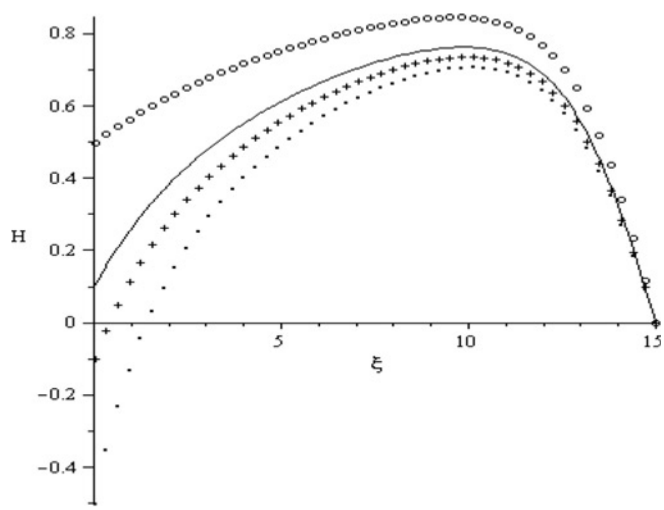

Notes: $Ec = 0.1$, $G_r = 0.1$, $Re = 1$, $M = 1$, $Da = 10$ and $s = 1$

Figure 10. Effect of varying H_w on axial velocity component

4.3 Effect of the Darcy number

The effect of the Darcy number on the flow characteristics has not been considered in the recent studies by Osalusi and his co-works (Frusteri and Osalusi, 2007; Osalusi and Sibanda, 2006; Osalusi *et al.*, 2007) nor in the earlier studies by Attia (for example, Attia, 2004, 2005, 2006, 2007; Attia and Aboul-Hassan, 2004). The effect of the Darcy number on the velocity components and temperature profile is illustrated in Figures 6-8. For high Darcy number (corresponding to high permeability), the fluid velocity attains a maximum at or near the surface. A decrease in the Darcy number results in a gradual decline in the boundary-layer velocity and a simple explanation for this is that a decrease in the permeability presents a physical barrier to the fluid flow.

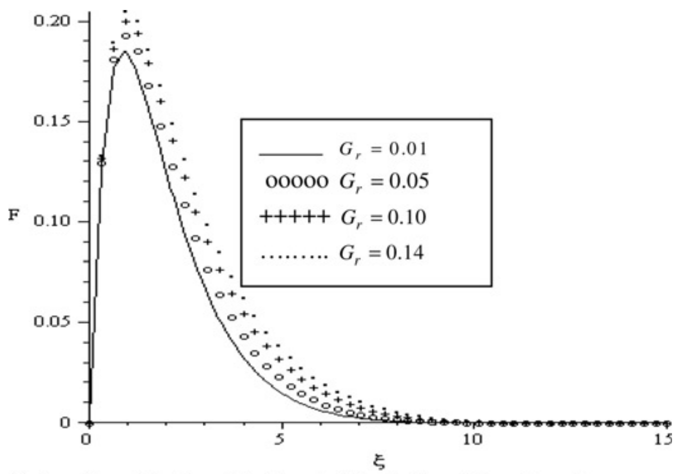

Notes: $Ec = 0.1$, $Da = 10$, $Re = 1$, $M = 1$, $H_w = 0.1$ and $s = 1$

Figure 11.
The effect of varying G_r on the radial velocity

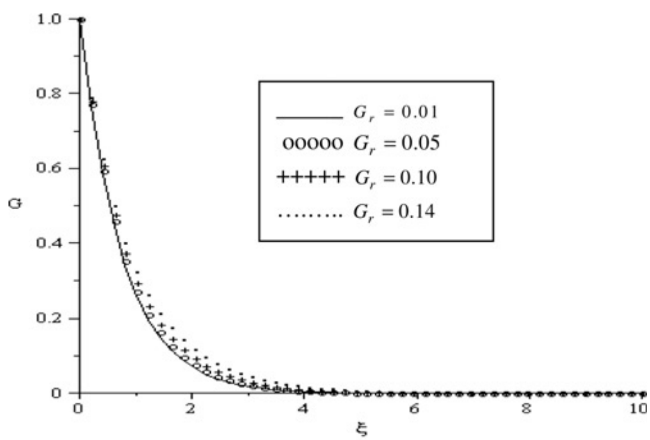

Notes: $Ec = 0.1$, $Da = 10$, $Re = 1$, $M = 1$, $H_w = 0.1$ and $s = 1$

Figure 12.
Effect of varying G_r on tangential velocity

Consequently, less fluid passes through the medium and, as expected, the fluid velocity decreases in all directions.

Analysis shows that increasing the Darcy number increases the boundary layer temperature.

4.4 Effect of suction and injection

The effect of the fluid suction and injection on the velocity components is illustrated in Figures 9 and 10.

4.5 Effect of Grashof number

The Grashof number G_r is a buoyancy term whose increase signifies an increase in the disk temperature T_w, thus enhancing free convection currents and a heating of the fluid

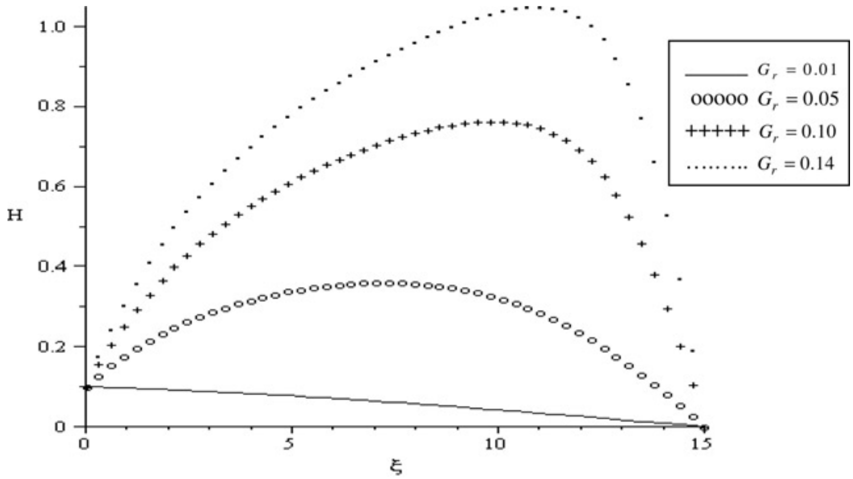

Notes: $Ec = 0.1$, $Da = 10$, $Re = 1$, $M = 1$, $H_w = 0.1$ and $s = 1$

Figure 13.
Effect of varying G_r on axial velocity

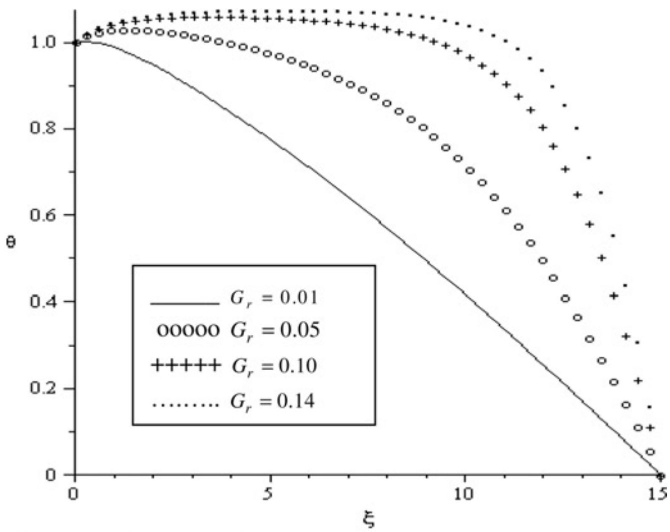

Notes: $Ec = 0.1$, $Da = 10$, $Re = 1$, $M = 1$, $H_w = 0.1$ and $s = 1$

Figure 14.
Effect of varying G_r on the temperature profiles

adjacent to the disk surface (as seen in Figure 11). As expected, the lighter warmer fluid then tends to spread faster in all directions. This increase in the velocity and temperature of the fluid is shown in Figures 13-16.

4.6 Effect of the Eckert number

Figures 15-17 show the influence of the Eckert number on the velocity components and the temperature distribution. The effect of increasing the Eckert number is to increase both the boundary-layer velocity and the temperature distribution.

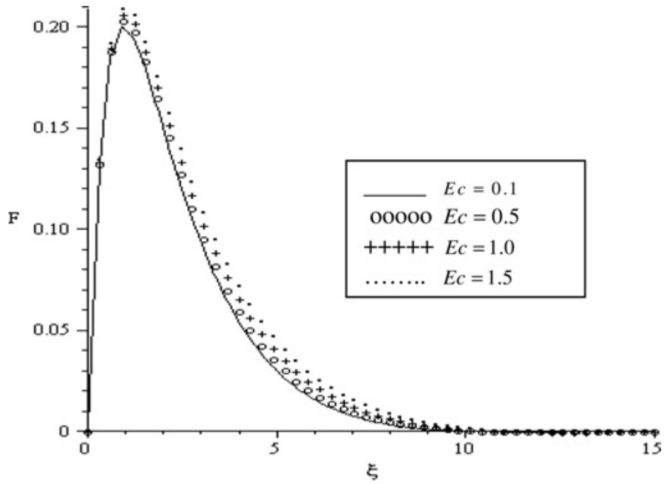

Notes: $G_r = 0.1$, $Da = 10$, $Re = 1$, $M = 1$, $H_w = 0.1$ and $s = 1$

Figure 15.
Effect of increasing the Eckert number *Ec* on radial velocity

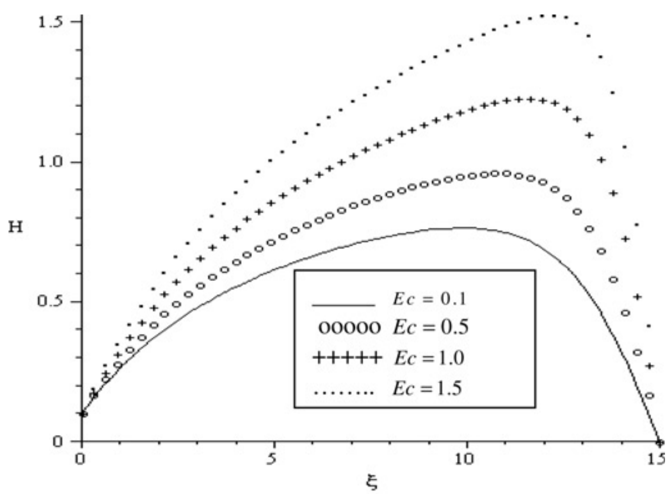

Notes: $G_r = 0.1$, $Da = 10$, $Re = 1$, $M = 1$, $H_w = 0.1$ and $s = 1$

Figure 16.
Effect of increasing the Eckert number *Ec* on axial velocity

4.7 Effect of the rotational Reynolds number

The rotational Reynolds number measures the strength of the rotation-induced flow and for higher *Re* the tangential and radial velocity components are enhanced while the axial velocity is suppressed. The temperature field also reduces with increasing speeds of rotation as shown in Figure 19.

5. Conclusion

We have investigated the heat transfer characteristics of steady MHD flow and heat transfer of viscous electrically conducting incompressible fluid with Hall current past a rotating disk with ohmic heating and viscous dissipation. This type of problem has potential to serve as a prototype for practical swirl problems, for example,

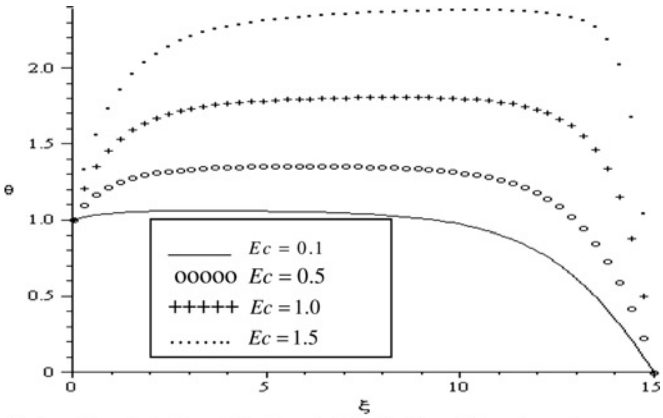

Notes: $G_r = 0.1$, $Da = 10$, $Re = 1$, $M = 1$, $H_w = 0.1$ and $s = 1$

Figure 17.
Effect of the Eckert number on the temperature profile

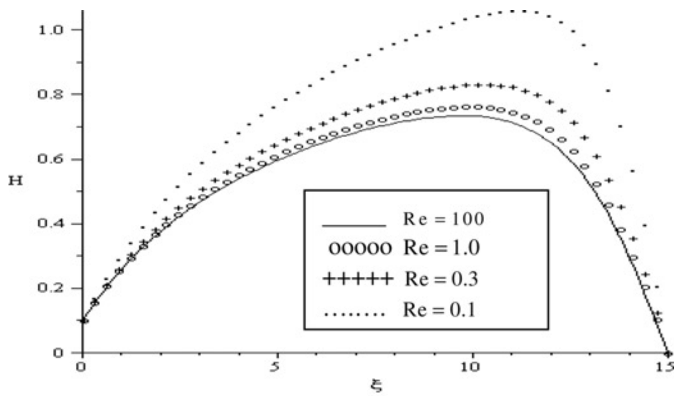

Notes: $G_r = 0.1$, $Da = 10$, $Ec = 0.1$, $M = 1$, $H_w = 0.1$ and $s = 1$

Figure 18.
Effect of increasing the Reynolds number *Re* on axial velocity

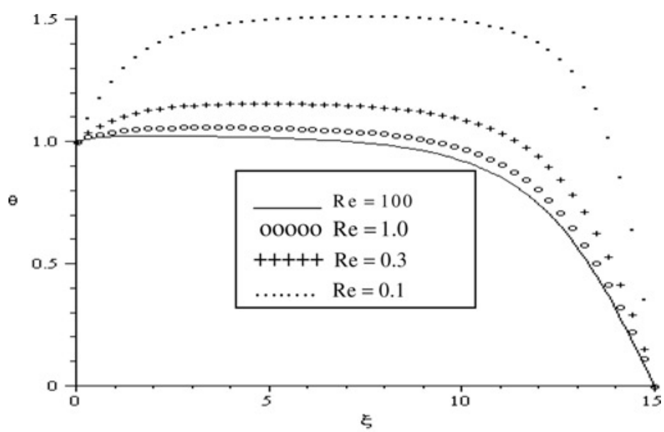

Notes: $G_r = 0.1$, $Da = 10$, $Ec = 0.1$, $M = 1$, $H_w = 0.1$ and $s = 1$

Figure 19.
Effect of increasing the Reynolds number *Re* on temperature profile

axisymmetric flow in combustors, see Kelson and Desseaux (2000). Numerical computations were carried out to study the effect of the various physical parameters controlling the system. The magnetic field retards the fluid motion due to the opposing Lorentz force generated by the magnetic force. An interesting finding in this study is that both the magnetic field and the Eckert number tend to enhance rather than degrade the heat transfer efficiency. The Hall parameter however reduces the heat transfer rate. In terms of the friction coefficient, the magnetic interaction parameter, the Hall parameter and the Eckert number all combine to increase the skin friction while increasing the Darcy number (increasing permeability) reduces the skin friction so increasing the fluid velocity.

References

Arikoglu, A. and Ozkol, I. (2006), "On the MHD and slip flow over a rotating disk with heat transfer", *International Numerical Journal of Heat and Fluid Flow*, Vol. 16 No. 2, pp. 172-84.

Attia, H.A. (2004), "Ion slip effect on the flow due to a rotating disk", *The Arabic Journal of Science and Engineering*, Vol. 29 No. 2A, pp. 165-72.

Attia, H.A. (2005), "MHD Couette flow with temperature dependent viscosity and the ion slip", *Tamkang Journal of Science and Engineering*, Vol. 8 No. 1, pp. 11-16.

Attia, H.A. (2006), "Unsteady flow and heat transfer of viscous incompressible fluid with temperature-dependent viscosity due to a rotating disc in a porous medium", *Journal of Physics A: Mathematical and General*, Vol. 39, pp. 979-91.

Attia, H.A. (2007), "Rotating disk flow and heat transfer of a conducting non-Newtonian fluid with suction-injection and ohmic heating", *Journal of the Brazilian Society of Mechanical Science and Engineering*, Vol. 19 No. 2, pp. 168-73.

Attia, H.A. and Aboul-Hassan, A.L. (2004), "On hydromagnetic flow due to a rotating disk", *Applied Mathematical Modelling*, Vol. 28, pp. 1007-14.

Benton, E.R. (1966), "On the flow due to a rotating disk", *Journal of Fluid Mechanics*, Vol. 24, pp. 781-800.

Cochran, W.G. (1934), "The flow due to a rotating disk", *Mathematical Proceedings of the Cambridge Philosophical Society*, Vol. 30 No. 3, pp. 365-75.

El-Mistikawy, T.M.A., Attia, H.A. and Megahed, A.A. (1990), "The rotating disk flow in the presence of a weak magnetic field", *Proceedings of the Fourth Conference on Theoretical and Applied Mechanics, Cairo, 5-7 November*, pp. 69-82.

Frusteri, F. and Osalusi, E. (2007), "On MHD and slip flow over a rotating porous disk with variable properties", *International Communications on Heat and Mass Transfer*, Vol. 34, pp. 492-501.

Herwig, H. (1985), "The effect of variable properties on momentum and heat transfer in a tube with constant heat flux across the wall", *International Journal of Heat Mass Transfer*, Vol. 28, pp. 424-41.

Herwig, H. and Klemp, K. (1988), "Variable property effects of fully developed laminar flow in concentric annuli", *ASME Journal of Heat Transfer*, Vol. 110, pp. 314-20.

Kelson, N. and Desseaux, A. (2000), "Note on porous rotating disk flow", *ANZIAM Journal*, Vol. 42 (E), pp. C847-55.

Makinde, O.D. (2005), "Free-convection flow with thermal radiation and mass transfer past a moving vertical porous plate", *International Communications in Heat and Mass transfer*, Vol. 32, pp. 1411-9.

Makinde, O.D. and Sibanda, P. (2008), "MHD mixed convective flow and heat and mass transfer past a vertical plate in a porous medium with constant wall suction", *ASME – Journal of Heat Transfer*, Vol. 130, pp. 112602-8.

Maleque, A.Kh. and Sattar, A.Md. (2005), "Steady laminar convective flow with variable properties due to a porous rotating disk", *Journal of Heat Transfer*, Vol. 127, pp. 1406-9.

Osalusi, E. and Sibanda, P. (2006), "On variable laminar convective flow properties due to a porous rotating disk in a magnetic field", *Romanian Journal of Physics*, Nos 9/10, pp. 933-44.

Osalusi, E., Side, J. and Harris, R. (2007), "The effects of Ohmic heating and viscous dissipation on unsteady MHD and slip flow over a porous rotating disk with variable properties in the presence of Hall and ion-slip currents", *International Communications on Heat and Mass Transfer*, Vol. 34, pp. 1017-29.

Rogers, M.G. and Lance, G.N. (1960), "The rotationally symmetric flow of a viscous fluid in presence of infinite rotating disk", *Journal of Fluid Mechanics*, Vol. 7, pp. 617-31.

Takha, H.S., Sing, A.K. and Nath, G. (2002), "Unsteady MHD flow and heat transfer on a rotating disk in an ambient fluid", *International Journal of Thermal Science*, Vol. 41, pp. 147-55.

von Karman, T. (1921), "Uber laminare und turbulente Reibung", *Zeitschrift fur Angewandte Mathematik und Mechanik*, Vol. 1, pp. 233-55.

Corresponding author
O.D. Makinde can be contacted at: makinded@cput.ac.za